

R8901269

I.P.N. BP n°1 - 91406 ORSAY

institut de physique nucléaire

CNRS - IN2P3 - UNIVERSITÉ PARIS - SUD



IPNO DRE 87-39

REVIEW OF HIGH EXCITATION ENERGY STRUCTURES IN HEAVY ION COLLISIONS : TARGET EXCITATIONS AND THREE BODY PROCESSES

N. FRASCARIA

Invited talk given at the first topical meeting on Giant Resonance Excitation in Heavy Ion Collisions, Legnaro, Italy (21-25 sept. 1987)

REVIEW OF HIGH EXCITATION ENERGY STRUCTURES IN HEAVY ION COLLISIONS : TARGET EXCITATIONS AND THREE BODY PROCESSES

N. Frascaria

Institut de Physique Nucléaire, BP 1, 91406 ORSAY CEDEX (France)

Abstract

A review of experimental results on high excitation energy structures in heavy ion inelastic scattering is presented. The contribution to the spectra of the pick-up break-up mechanism is discussed in the light of the data obtained with light heavy ion projectiles. Recent results obtained with ^{40}Ar beams at various energies will show that target excitations contribute strongly to the measured cross section.

1. INTRODUCTION

The excitation of collective modes is expected to play important roles in many aspects of the dynamics of nucleus-nucleus collisions. The most direct evidence for the excitations of such states should come from the study of inelastic scattering. Ten years ago, first evidence for the presence of structures at high excitation energy in the inelastic channel from some heavy ion reactions was reported. However due to the complexity of heavy ion reaction mechanisms it was not straightforward to interpret these structures since they could be due not only to nuclear excitations but also to many body processes such as pick-up break-up reactions. In the last few years a large amount of theoretical and experimental work has allowed us to progress towards a deeper understanding of these inelastic spectra.

This paper shall be devoted to a review of the most recent experimental results. In parts 2 and 3 the results obtained at low incident energy and the first results obtained at GANIL at intermediate energy will be reviewed in order to show the presence of physical structures in the high excitation energy region. In the two following parts I will present experiments with "light" heavy ion projectiles in which effects of three body processes can be observed and will be discussed. In the last part, preliminary results obtained at GANIL with the SPEG spectrograph will show that the use of a heavy beam such as ^{40}Ar allows the observation of structures due to target excitations superimposed on the three body continuum.

2. EXPERIMENTAL OBSERVATIONS AT LOW INCIDENT ENERGY

An important amount of work has been done at low incident energies from 4 MeV/n to 11 MeV/n¹⁻⁸; the study of symmetric systems followed by the study of very asymmetric systems, inclusive experiments and coincidence experiments. These results are now published^{1,2,5} and I would like just to review the main characteristics of the structures. At these low incident energies :

- the structures are observed in the inelastic and few nucleon transfer channels for angles near or slightly before the grazing angle.
- their positions are independent of angle.
- their width increases with excitation energy.
- the structures at low excitation energy ($E_x \leq 40$ MeV) are peaked at the grazing angle while the ones at $E_x \geq 40$ MeV are more forward peaked.
- In the $^{40}\text{Ca} + ^{40}\text{Ca}$ reaction studied at 4, 7 and 10 MeV/n, the positions of the bumps are independent of incident energy in the energetically allowed excitation energy range.

All these experimental features suggest that the structures corresponding to well defined excitation energies are excited mainly through a direct process and that we are dealing with an excitation of the target nucleus. However the data concerning these structures were restricted to a limited number of systems and bombarding energies and more systematic studies were necessary to resolve several questions concerning their nature.

3. FIRST EXPERIMENTAL RESULTS WITH AN Ar BEAM AT INTERMEDIATE ENERGY

From DWBA calculations giant resonance cross sections from heavy ion inelastic scattering are expected to be considerably enhanced at high incident energy. If the high energy structures can be related to collective excitations one way to get a deeper insight into their excitation mechanism is to perform experiments at higher incident energies. The giant resonances are known to be a general property of nuclei. Thus a better knowledge of the evolution of these structures with mass number is required. Therefore we have performed experiments at GANIL at intermediate energy.

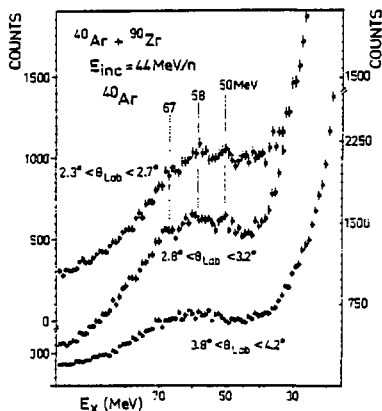


Fig. 1. Inelastic $^{40}\text{Ar} + ^{90}\text{Zr}$ spectra obtained at 3 different angles presented in a linear scale with 1 MeV/channel-binning.

A first step was the study of the $^{40}\text{Ar} + ^{40}\text{Ca}$, ^{90}Zr , ^{120}Sn and ^{208}Pb reactions at 44 MeV/n using a time of flight spectrometer built for these experiments ⁷. Data were taken for angles close to the grazing angle in each reaction. In fig.(1) are displayed three inelastic $^{40}\text{Ar} + ^{90}\text{Zr}$ spectra obtained at different angles around the grazing angle ($\theta_{gr} = 2.9^\circ$). At angles close to and slightly before the grazing the bumps show up clearly in the spectra up to 60 MeV and they are best observed at forward angles. A very rapid decrease with angle is observed for the structures and for large angles ($\approx 4^\circ$) they have completely disappeared.

These structures have a small cross section and are superimposed on a large physical background. In order to obtain more quantitative information on the high energy structures statistical analyses such as auto-correlation and cross-correlation analyses were carried out on the inelastic energy spectra of the $^{40}\text{Ar} + ^{90}\text{Zr}$ reaction following the methods developed in ref. 8. In these calculations, the structures are analyzed as fluctuations around an average cross section which is defined by the sliding average method.

$$\langle \sigma(E_i) \rangle = \frac{1}{2\Delta + 1} \sum_{j=i-\Delta}^{i+\Delta} \sigma(E_j)$$

where Δ corresponds to an averaging interval of ± 6 MeV in the present case. The auto correlation function is then defined by

$$C(\varepsilon) = \left\langle \left(\frac{\sigma(E+\varepsilon) - \langle \sigma(E+\varepsilon) \rangle}{\langle \sigma(E+\varepsilon) \rangle} \right) \left(\frac{\sigma(E) - \langle \sigma(E) \rangle}{\langle \sigma(E) \rangle} \right) \right\rangle$$

In fig. (2) is displayed the result of the auto-correlation calculations for different energy spectra over the excitation energy range $36 < E^* < 82$ MeV. In such a correlation function the first channel corresponding to the correlation between two unshifted spectra indicates the strength of statistical fluctuations. For small angles the first shoulder observed in the correlation functions demonstrates the presence of structures in the spectra. The strong bump centered around $\varepsilon = 9$ MeV shows that the experimental structures are regularly spaced by about 9 MeV. Even if the correlation becomes rather weak the presence of the following bump centered around $\varepsilon = 20$ MeV indicates that at least three structures are present in the studied excitation energy range of the original spectra. At angles larger than about 3.8° where the structures are not seen in the experimental spectra the correlation function exhibits (see fig. (2.1)) a very different pattern. None of the above features is observed.

A cross correlation analysis has been carried out following the same method in order to obtain the degree of correlation of the structures observed in the spectra taken at different angles (see fig.(2.2)). The cross correlation analysis was done by shifting the first spectrum with respect to the second one in order to find the different cross correlation maxima. These maxima are related to different bumps in the spectra and their position gives the average spacing between the bumps. In fig. (2.2) three cross correlation maxima are clearly observed in all cross correlation curves. Again the average spacing between

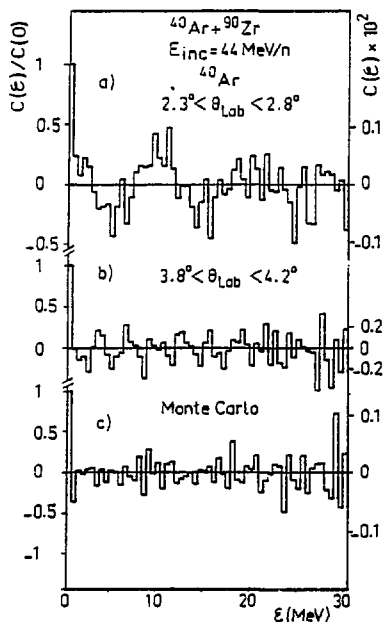


Fig. 2.1

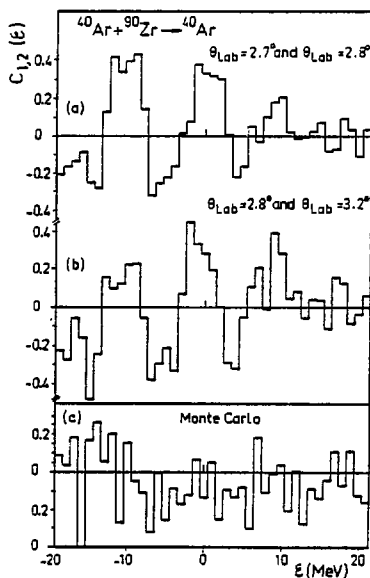


Fig. 2.2

Fig. 2.1. Auto-correlation functions for two $^{40}\text{Ar} + ^{90}\text{Zr}$ inelastic spectra and for a random fluctuation spectrum (see ref. 7).

Fig. 2.2. Cross-correlation functions for $^{40}\text{Ar} + ^{90}\text{Zr}$ inelastic spectra
 a) between $\theta_{\text{Lab}} = 2.7^\circ$ and $\theta_{\text{Lab}} = 2.8^\circ$ b) between $\theta_{\text{Lab}} = 2.8^\circ$ and $\theta_{\text{Lab}} = 3.2^\circ$
 c) between two random fluctuation spectra (see ref. 7).

these maxima is around 10 MeV which is in agreement with the auto-correlation analysis. Moreover the fact that the cross correlation functions exhibit a maximum for $\epsilon = 0$ indicates that the structures lie at the same excitation energies, at all angles where they are observed.

In conclusion, these analyses quantitatively confirm the existence of physical structures regularly spaced in the excitation energy range of 36 to 82 MeV. As mentioned before, to understand the mechanism of excitation of these physical structures the knowledge of the evolution of the structures with incident energy and with target mass is primordial.

A first attempt consisted in the study of the influence of the target. The inelastic scattering of 44 MeV/n ^{40}Ar from ^{40}Ca , ^{90}Zr , ^{120}Sn and ^{208}Pb targets has been investigated and the resulting spectra are displayed in fig.(3). Structures are observed in the high excitation energy region in all inelastic channels. These structures are not found at the same excitation energies in the four spectra. The structures seem to be a general property of nuclei and clearly evolve as a function of the target mass. This point will be developed later.

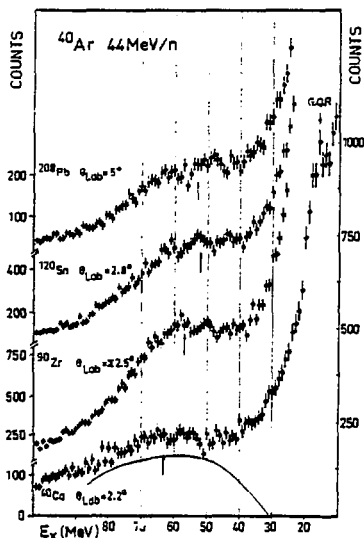


Fig. 3. Inelastic ^{40}Ar spectra from ^{208}Pb , ^{90}Zr and ^{40}Ca presented in linear scale with 1MeV/channel binning. (for more details see ref. 7)

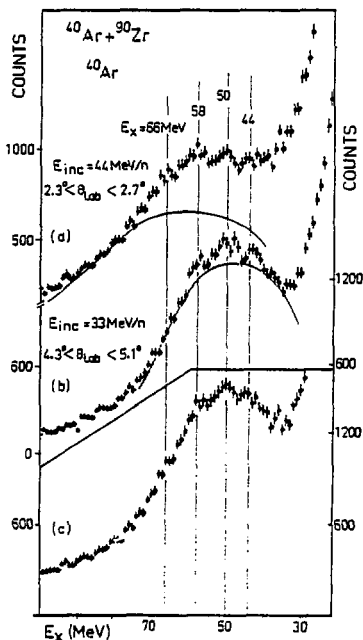


Fig. 4. Inelastic $^{40}\text{Ar} + ^{90}\text{Zr}$ spectra measured a) at 44 MeV/n b) at 33 MeV/n. Spectrum c) illustrates the effects of the different backgrounds (see ref. 7).

where $\langle \bar{E}_s \rangle$ is the average kinetic energy of the emitted light particle in the frame of the projectile-like fragment, $S_3(4')$ is the separation energy of the light particle in the target and E_T^* is the excitation energy of the target-like nucleus.

From these formulae we can deduce that E_{up}^* depends very little on the nature of the target. Thus for a given projectile at a given incident energy, the pick-up break-up contribution is nearly the same for reactions on different targets. The most important term in these formulae is the one proportional to E_{lab}/M_3 which implies that E_{up}^* and Γ depend strongly on the beam energy per nucleon. Thus a variation of the bombarding energy can provide an unambiguous discrimination between target excitation and decay products of excited projectile fragments. This is an important point for the following.

In order to describe in detail the energy spectra of the various transfer evaporation channels a Monte Carlo calculation has been performed⁹ for the studied reactions using the code LILITA¹⁰ which assumes a purely statistical decay process in the framework of the Hauser Feshbach theory where the light particles are emitted isotropically in the cm of the fully accelerated fragment. As the first step of the reaction is not known, this calculation necessitates several assumptions which are discussed in detail in ref 9. Fig. (5) displays the inelastic $^{40}\text{Ar} + ^{90}\text{Zr}$ spectrum compared to the result from the LILITA calculation. In this calculation all the evaporation channels have been taken into account. The resulting curve is normalized to the experimental spectrum in order to indicate the maximum contribution consistent with the data. From this comparison, one can conclude that :

i) the widths of the calculated contributions are much larger than the ones of the observed structures and thus this process contributes only to the background of the spectra

ii) the evaporation channels of more than one nucleon contribute to a region where the experimental cross section is very small and where no structures are observed.

Before going into the details of the most recent results obtained at GANIL, let me present and discuss results from other laboratories using "light" heavy ion beams.

5. EXPERIMENTAL RESULTS WITH "LIGHT" HEAVY ION PROJECTILES

Recently several studies of inelastic scattering of light heavy ions at intermediate

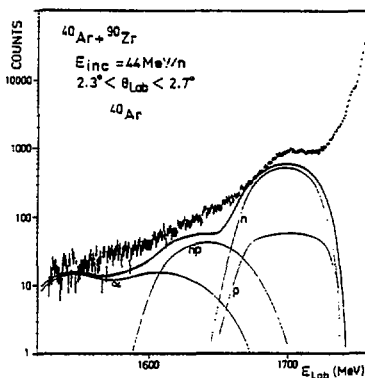


Fig. 5. Comparison of the inelastic $^{40}\text{Ar} + ^{90}\text{Zr}$ spectrum with the pick-up break-up calculation described in text.

energy have been performed. Two of them, the studies of the $^{20}\text{Ne} + ^{208}\text{Pb}$ reaction¹¹ at 30 MeV/n and of $^{17}\text{O} + ^{208}\text{Pb}$ at 22 MeV/n¹² concluded to the absence of physical structures in the high excitation energy region. However these conclusions must be taken with caution since in both experiments several structures were observed but attributed to defects in the detection systems and moreover a very recent study¹³ of ^{20}Ne inelastic scattering on ^{208}Pb has demonstrated that the conclusions of ref. 11 were incorrect and that physical bumps are present in the $^{20}\text{Ne} + ^{208}\text{Pb}$ spectra at 30 MeV/n.

Let me now present and discuss the two recent experiments $^{16}\text{O} + ^{208}\text{Pb}$ performed at 22 and 25 MeV/n (Oak Ridge)¹⁴ and $^{20}\text{Ne} + ^{208}\text{Pb}, ^{90}\text{Zr}$ at 25 and 30 MeV/n (MSU)¹³.

5.1. The $^{16}\text{O} + ^{208}\text{Pb}$ experiment¹⁴

This reaction was studied at two slightly different incident energies. In fig. 6 are displayed the two inelastic channels from this reaction at 22 and 25 MeV/n. Together with the G.Q.R. and two peaks at 13.6 and 17 MeV two bumps are observed at approximately 25 and 40 MeV excitation energies. These two bumps have a cross section only a factor ~ 2 smaller than the GQR and between the two experiments their excitation energies are shifted by ~ 2.5 MeV. Clearly these structures cannot be identified with high excitation energy states of the target nucleus since the observed shift follows the kinematical evolution predicted for a pick-up break-up reaction. Obviously the pick-up break-up component calculated with LILITA as described in paragraph 4 cannot reproduced the two observed bumps. This point will be discussed in section 5.3.

5.2. The $^{20}\text{Ne} + ^{208}\text{Pb}, ^{90}\text{Zr}$ experiment¹³

The inelastic scattering of ^{20}Ne on ^{90}Zr and ^{208}Pb has been studied at 500 and 600 MeV incident energies. High statistics spectra were measured at the grazing angle using a magnetic spectrograph. In fig. (7) are displayed the inelastic spectra obtained in these reactions. In the case of the Pb target, structures are clearly observed in the inelastic spectra at the two incident energies but they appear at different excitation energies. A cross correlation analysis of these data was carried out for both studied systems. In the case of the $\text{Ne} + \text{Pb}$ system, the cross correlation function is strongly negative for unshifted spectra, indicating that the structures observed at 600 MeV and 500 MeV incident energies are out of phase (see fig. 8). It takes its maximum when one of the spectra is shifted by about 5 MeV relative to the other. Again this corresponds exactly

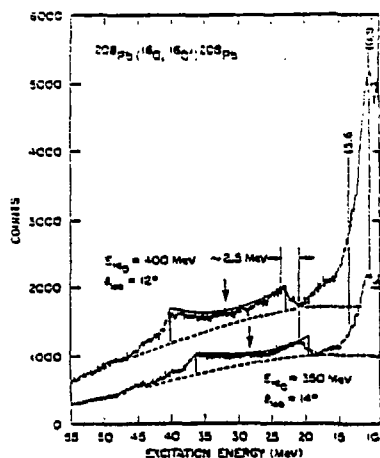


Fig. 6. Inelastic spectra from $^{16}\text{O} + ^{208}\text{Pb}$ reaction from ref. 14. The solid line represents the calculation of the double humped pick-up break-up component arbitrarily normalized to the data (see text).

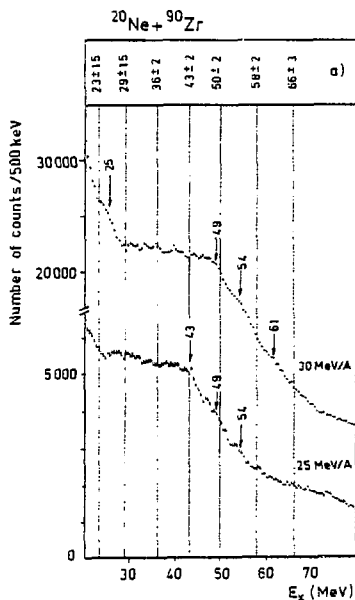
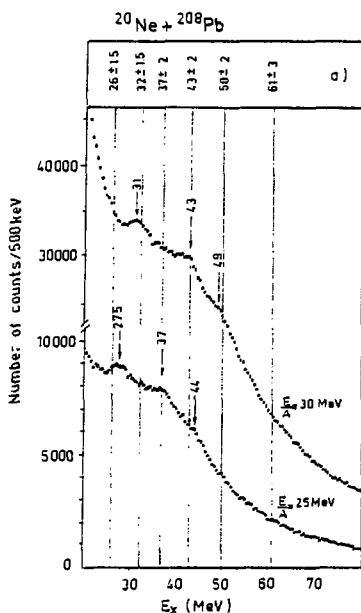


Fig. 7. Inelastic scattering spectra at the grazing angle from the reactions $^{20}\text{Ne} + ^{208}\text{Pb}$ and $^{20}\text{Ne} + ^{90}\text{Zr}$ at 500 and 600 MeV incident energies (for more details see ref. 13).

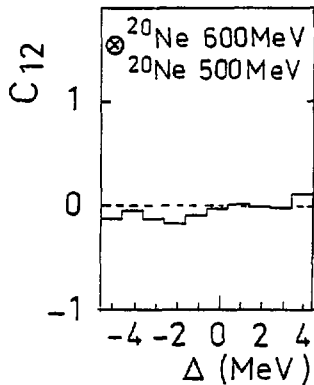
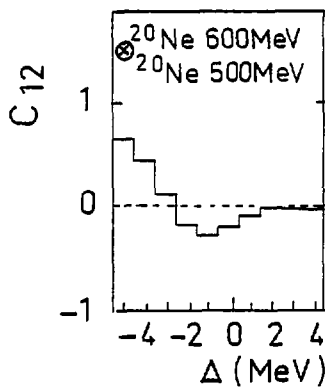


Fig. 8. Cross-correlation functions between the spectra taken at 25 MeV/n and 30 MeV/n for the $^{20}\text{Ne} + ^{208}\text{Pb}$ (a) and $^{20}\text{Ne} + ^{90}\text{Zr}$ (b) reactions.

to what is expected from a quasi projectile excitation. A different result is obtained for the $^{20}\text{Ne} + ^{90}\text{Zr}$ inelastic spectra. The correlation function is rather flat and close to zero for unshifted spectra (see fig. 8).

Let me now discuss these results in terms of pick-up break-up effects.

5.3. Discussion

In the pick-up break-up calculations discussed in the preceding paragraph, continuous excitation energy and spin distributions were postulated for the levels excited just above the emission threshold of the quasi projectile. If now we assume that due to momentum matching conditions a level just above the particle emission threshold is highly excited in the quasi-projectile giving rise to a strong angular momentum alignment the light particles will be emitted following a Legendre Polynomial $P_{Lm}(\cos \theta)$ distribution. A complete calculation⁹ shows that the transfer evaporation contribution is then split into two peaks separated by the width Γ . This double humped contribution follows the same evolution with incident energy and target mass as described before for the flat pick-up break-up component.

In the case of the $^{16}\text{O} + ^{208}\text{Pb}$ reaction, if we assume that the $\frac{3}{2}^+ L = 2$ level at 5.08 MeV is strongly excited in ^{17}O with an aligned angular momentum one can reproduce completely the data⁹ (fig. (6)). As already observed in the $^{16}\text{O} + ^{208}\text{Pb}$ experiment the shift between the two main bumps observed at 25 MeV/n and 30 MeV/n in the $^{20}\text{Ne} + ^{208}\text{Pb}$ inelastic channel roughly corresponds to the difference between the two incident energies per nucleon. A complete pick-up break-up calculation shows that these peaks could correspond to the decay of an unbound state in ^{21}Ne which emits a neutron of 0.4 MeV (see ref. 13).

One can notice that this phenomenon occurs for quasi projectiles such as ^{17}O and ^{21}Ne having a low level density above the emission threshold. In the case of heavy quasi projectiles such as ^{41}Ar discussed before, the neutron threshold is high and the level density above this threshold is very large. Consequently in that case the probability to excite preferentially discrete states in the region above the emission threshold is certainly small. But it is not straightforward to appraise the probability of the presence of this double humped structure. It has been shown that, whether double humped structures are present or not, the centroid and the width of the pick-up break-up contribution depend strongly on the beam energy per nucleon. Thus, a clean method to conclude between target excitation and pick-up break-up reactions is to study a given system at two different incident energies. Even in this case the change of matching conditions between two very different incident energies could modify the relative population of the quasi projectile states. Consequently a definite conclusion concerning such a mechanism requires a comparison of two experiments where the bombarding energy per nucleon is varied by approximately half of the mean interval between two observed bumps.

6. S.P.E.G EXPERIMENTS

In this paragraph, let me present very recent and preliminary data we have obtained

at GANIL using the magnetic spectrograph SPEG. The aim of this experiment was to compare with high resolution and high statistics the inelastic scattering of ^{40}Ar on ^{90}Zr at 41 MeV/n and 44 MeV/n in order to distinguish between excitations of the projectile and the target fragments. The momentum range of the spectrograph is sufficiently large so that the entire excitation energy range of interest (≈ 100 MeV) could be covered at one magnetic field setting. The total aperture of the spectrograph is 4° . The emitted fragments were detected by the standard focal plane detection system consisting of two drift chambers for position measurements and two multi-anode ionisation chambers for particle identification. A time of flight measurement was taken between a large area parallel plate counter and the cyclotron R.F. An unambiguous mass, atomic and nuclear charge identification of the fragments in the vicinity of ^{40}Ar was obtained.

The first remarkable result of this experiment is the large peak to continuum ratio

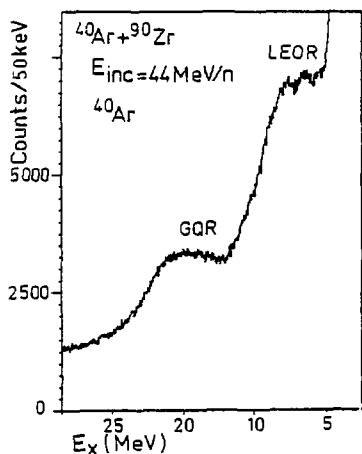


Fig. 9. Low excitation energy region ($0 < E_x < 20$ MeV) of the inelastically scattered ^{40}Ar spectrum from ^{90}Zr taken at the grazing angle.

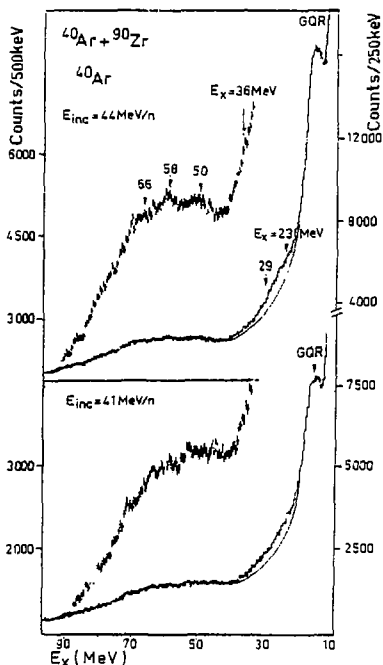


Fig. 10. Inelastic $^{40}\text{Ar} + ^{90}\text{Zr}$ spectra measured a. 41 MeV/n and 44 MeV/n with SPEG with two different representations (see text). The arrows indicate the positions of the bumps observed in the time of flight measurement at 44 MeV/n for the same system.

observed for the giant quadrupole resonance which is considerably enhanced at the studied energy compared to heavy ion experiments at lower incident energy (see fig. 9). In fig. (10) are displayed the two inelastic spectra at 44 MeV/n and 41 MeV/n incident energies, both with two different energy binnings : 250 keV/channel and 500 keV/channel in order to observe more clearly the broad structures at high excitation energy. At first glance the spectra at both incident energies are very similar and exhibit structures up to ~ 60 MeV excitation energy.

In order to insure that these small cross section fluctuations are not due to differential non linearities of the position sensitive drift chambers measurements were performed with three different settings of the magnetic field of the spectrograph at both incident energies. To check the consistency of the excitation energy spectra at different ($B\rho$) cross

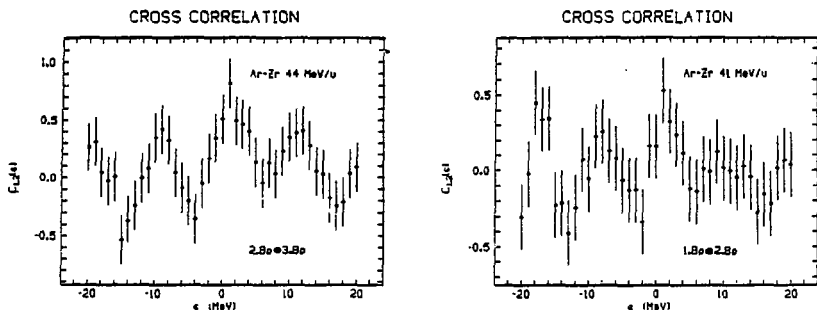


Fig. 11. Cross-correlation functions between spectra taken at two different settings of the magnetic field : on the left at 44 MeV/n, on the right at 41 MeV/n. The errors bars are calculated following ref. 8.

correlation analyses were carried out and are displayed in fig. (11). The fact that the cross correlation functions show a maximum for $|\epsilon| < 1$ MeV clearly demonstrates that the main oscillations observed in the spectra have a physical origin. The uncertainty of the energy calibration is estimated to be less than 1 MeV.

Now, we shall compare the two inelastic spectra obtained at 44 MeV/n and 41 MeV/n (fig. (12)). These spectra are preliminary and the full statistics have not yet been analysed. Nevertheless the result is clear : the bumps are not shifted and show up at the same position in both spectra. In the upper part of fig. (12), these two spectra are summed for a same number of counts and in the resulting spectrum the three observed bumps remain. Moreover a cross correlation analysis between the two spectra taken at 44 MeV/n and 41 MeV/n has been carried out. As one can see in fig. (13) a strong maximum is observed for the unshifted spectra ($\epsilon = 0$) showing that the structures are in phase at both incident energies.

A supplementary test to show the accuracy of this result is given by the comparison

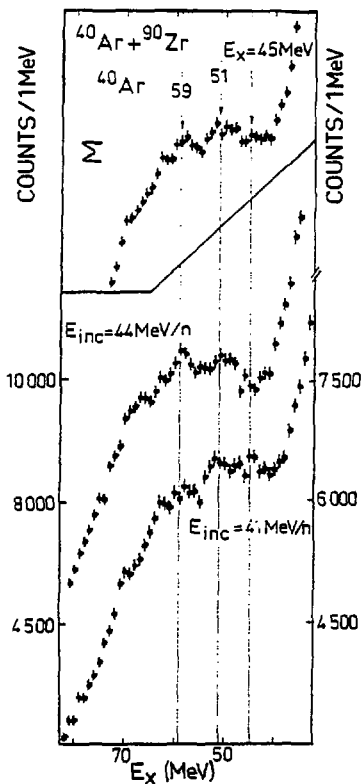


Fig. 12. Lower part : comparison between the inelastic spectra from the $^{40}\text{Ar} + ^{90}\text{Zr}$ reaction measured at 44 MeV/n and 41 MeV/n. Upper part : sum of a 41 MeV/n and 44 MeV/n spectrum having both approximately the same number of counts.

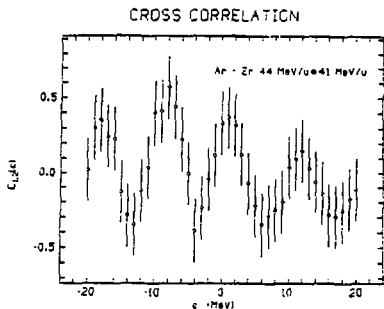


Fig. 13. Cross-correlation function between the two spectra of the lower part of fig. 12.

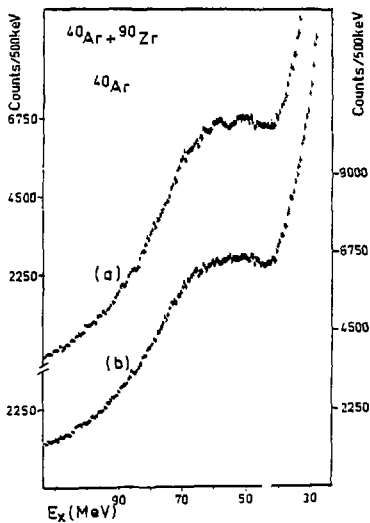


Fig. 14. a) target excitation case : same as upper part of fig. 12 with a different energy binning b) quasi-projectile case (see text).

of the two spectra displayed in fig. 14. Spectrum a) is obtained by summing the spectra at 44 and 41 MeV/nucleon for a same number of counts. The bumps observed in these two spectra are clearly visible in the sum spectrum a) which is expected if they are due to target excitation. On the other hand structures produced by pick-up break-up reactions are expected to shift by 3 MeV between 44 and 41 MeV/n (see paragraph 4). To investigate this last hypothesis, spectrum b) presents the sum of the 44 MeV/n data and the 41 MeV/n spectrum shifted upwards in excitation energy by 3 MeV. Within the statistical error bars spectrum b) is flat showing that the contribution to the structures of double humped pick-up break-up components, if it exists at all, is very weak. Moreover the structureless spectrum obtained in this case shows that the 3 MeV/n energy shift between the two incident energies provides a meaningful test to conclude between target excitations and three body reactions.

In fig. (15) are displayed the four inelastic spectra obtained in the $Ar + Zr$ reaction

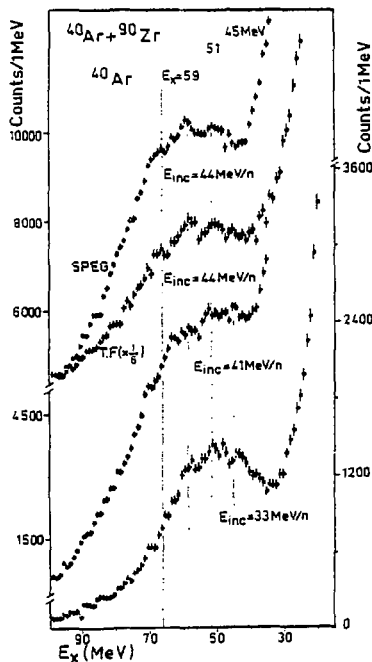


Fig. 15. Comparison between the inelastic spectra from the $^{40}Ar + ^{90}Zr$ reaction measured at 33 MeV/n (time of flight measurement), 41 MeV/n (SPEG measurement) and 44 MeV/n using the two different set ups.

at 33 MeV/n, 41 MeV/n and 44 MeV/n with two different set ups - the time of flight (TF) discussed previously and SPEG. Clearly the bumps show up at the same position at the three different incident energies. One can notice that the two spectra obtained with TF and SPEG are identical and differ only by the number of counts which is a factor 6 larger in the SPEG experiment.

7. DISCUSSION

If we recapitulate now all the data obtained with the ^{40}Ar beam at GANIL it has been shown that i) in the case of the Zr target the positions of all the structures are confirmed with high statistics in the SPEG experiment. This gives confidence in the time of flight measurements presented before ii) the results obtained at 33 MeV/n, 41 MeV/n and 44 MeV/n for the Ar + Zr reaction point to an interpretation of the structures in terms of target excitation iii) a clear evolution of the structures with target mass is observed.

Thus, from the time of flight data we have tried to extract the different positions of these bumps in the four studied systems. Different methods have been used (see ref. 7) consisting in different background subtractions and a double Fourier transform analysis. A compilation of these results taking into account all the measured angles is shown in fig. (16). The error bars reflect the dispersion on the excitation energies given by the different

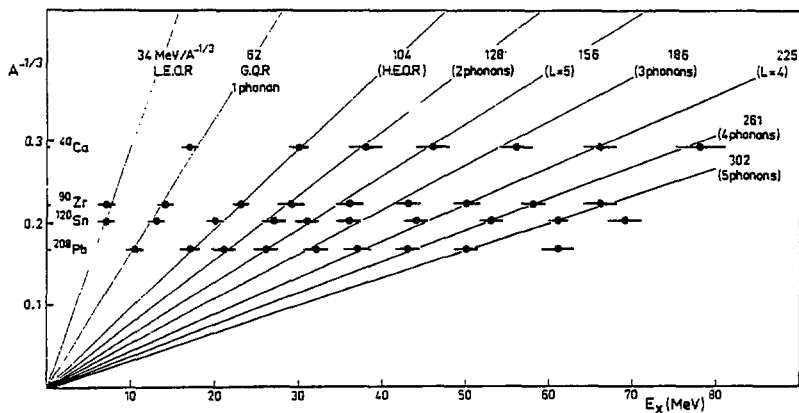


Fig. 16. Excitation energies of the structures observed in the inelastic channels of the four reactions ($^{40}\text{Ar} + ^{40}\text{Ca}$, $^{90}\text{Ar} + ^{90}\text{Zr}$, $^{120}\text{Ar} + ^{120}\text{Sn}$, $^{208}\text{Ar} + ^{208}\text{Pb}$) plotted as a function of target mass $A^{-1/3}$. Tentative interpretations of the different states are given.

analyses and the uncertainties due to statistical fluctuations and energy calibrations. An attempt was made to reproduce the positions of the structures with different laws of the type $E_x \propto A^P$ but the only consistent representation of the data is given by $A^{-1/3}$ laws as

presented in fig. (16). In such a representation, the points can be joined with surprising consistency by straight lines passing through 4 data points and the origin. The slopes of these lines in units of $\text{MeV}/A^{-1/3}$ are also indicated. The second slope corresponds to the well known G.Q.R. The first and the third ones can be tentatively associated with the low excitation and the high excitation octupole resonances (LEOR and HEOR). The others are not known and we can try to conjecture what might be the nature of these excitations.

To understand the origin of these bumps a large amount of theoretical work has been carried out during these last years ⁷. Up to now the most consistent representation of the data is given by the multiphonon calculation ^{6,15} where one supposes the excitation of multiphonon states built with the giant quadrupole resonance. This implies that the multiphonon energies are multiples of the G.Q.R. energy. As one can see in fig. (16) the 128, 186 and 261 $\text{MeV}/A^{-1/3}$ slopes are in surprisingly good agreement with such a picture corresponding respectively to what is predicted for 2, 3 and 4 phonons but all the data cannot be completely interpreted by this model and the nature of these structures remains an open question.

8. CONCLUSION

From the presented work, we have learned that projectile effects can be very important in some heavy ion collisions using "light" heavy ion projectiles leading to a highly excited double humped structure in the inelastic spectra. Consequently, if small target excitations are present in the spectrum this effect will not allow to observe them. With a heavy projectile such as ⁴⁰Ar, it has been shown that structures are observed in all studied target nuclei and these data are consistent with an excitation of the target. Light particle-heavy fragment coincidence experiments should now provide a unique tool to disentangle the contributions of projectile and target excitations in heavy ion inelastic spectra and will allow a further step towards the understanding of these complex reaction mechanisms.

Acknowledgements : I wish to acknowledge my colleagues D. Beaulieu, Y. Blumenfeld, Ph. Chomaz, J.P. Garron, J.C. Roynette, T. Suomijärvi, J. Barrette, B. Berthier, B. Fernandez, J. Gastebois and W. Mittig for many fruitful discussions and for allowing me to present our unpublished results. Special thanks are due to Y. Blumenfeld for a careful reading of the manuscript. I acknowledge D. Grialou for the elaboration of the manuscript.

References

- 1) N. Frascaria, C. Stéphan, P. Colombani, J.P. Garron, J.C. Jacmart, M. Riou, L.

Tassan-Got, Phys. Rev. Lett. 39(1977)918

- 2) N. Frascaria, P. Colombani, A. Gamp, J.P. Garron, M. Riou, J.C. Roynette, C. Stéphan, A. Ameaume, C. Bizard, M. Louvel, Z. Phys. A294 (1980) 167
N. Frascaria, Proceedings of the Int. Conf. on Nucl. Phys. (Trieste), Nucl. Phys. C.H. Dasso, R.A. Broglia, A. Winther EDS North Holland, Amsterdam (1982) 617
- 3) A.C. Mignerey, K.L. Wolf, M. Breuer, B.G. Glagola, V.E. Viola, J.B. Birkelund, D. Hilscher, J.R. Huizenga, W.V. Shroeder, W.W. Wilcke, Proc. of the Int. Conf. on Nucl. Phys., Berkeley, California (1980)
- 4) S. Pontoppidan, P.R. Christensen, D. Hansen, F. Videback, H.C. Britt, B.H. Erkkiza, Y. Patin, R.H. Stokes, M.P. Webb, R.L. Ferguson, E. Plasil, G.R. Young, Phys. Rev. C 28 (1983) 2299
- 5) Ph. Chomaz, N. Frascaria, Y. Blumenfeld, J.P. Garron, J.C. Jacmart, J.C. Roynette, W. Bohne, A. Gamp, W. von Oertzen, M. Buenerd, D. Lebrun and Ph. Martin, Z. Phys. A318 (1984) 41
- 6) Ph. Chomaz, Y. Blumenfeld, N. Frascaria, J.P. Garron, J.C. Jacmart, J.C. Roynette, W. Bohne, A. Gamp, W. von Oertzen, N.V. Giai and D. Vautherin Z. Phys. A 319 (1984) 167
Ph. Chomaz, thèse de 3ème cycle, IPNO Th 84-01
- 7) N. Frascaria, Y. Blumenfeld, Ph. Chomaz, J.P. Garron, J.C. Jacmart, J.C. Roynette, T. Suomijärvi and W. Mittig, Nucl. Phys. A474 (1987) 253 and references therein
- 8) P.J. Dallimore and I. Hall, Nucl. Phys. 88 (1966) 193
A. Richter, Nuclear Spectroscopy and reactions, Academic Press New York and London, 1974
M.G. Kendall and A. Stuart, Advanced theory of statistics, vol. 3, London (1976) 3rd ed.
- 9) Y. Blumenfeld, J.C. Roynette, Ph. Chomaz, N. Frascaria, J.P. Garron and J.C. Jacmart, Nucl. Phys. A 445 (1985) 151
- 10) J. Gomez del Campo and R. Stokstad, Oak Ridge, National Laboratory, report ORNL TM 7295
- 11) M. Buenerd, J. Chauvin, G. Duhamel, J.Y. Hostachy, D. Lebrun, P. Martin, P.O. Pellegrin, G. Perrin and P. de Saintignon, Phys. Lett. 167B (1986) 379
- 12) F.E. Bertrand, R.O. Sayer, R.L. Auble, M. Beckerman, J.L. Blankenship, B.L. Burks, M.A.G. Fernandes, C.W. Clover, E.E. Gross, D.J. Horen, J. Gomez del Campo, D. Shapira and H.P. Morsch, Phys. Rev. C35 (1987) 111

- 13) S. Fortier, S. Galès, S.M. Austin, W. Benenson, G.W. Crawley, C. Djalali, J.H. Lee, J. Van der Plicht and J.S. Winfield, Report IPNO DRE 87-22, Orsay (1987) and to be published in Phys. Rev. C
- 14) T.P. Sjoreen, F.E. Bertrand, R.L. Auble, E.E. Gross, D.J. Horen, D. Shapira and D.B. Wright, Phys. Rev. C29 (1984) 1370
- 15) Ph. Chomaz, N.V. Giai and D. Vautherin, Preprint IPNO Th 86-32 Orsay (1986), Nucl. Phys. (to be published) and references therein.